Available online at www.sciencedirect.com
SCIENCE DIRECT
Dyes and Pigments 72 (2007) 8–15
DYES and PIGMENTS
www.elsevier.com/locate/dyepig

Design, synthesis, and characterization of new iron-complexed azo dyes

Malgorzata Szymczyk, Ahmed El-Shafei, Harold S. Freeman*

Department of Textile Engineering, Chemistry and Science, Fiber and Polymer Science Program, North Carolina State University, Box 8301, Raleigh, NC 27695, USA

Received 28 March 2005; received in revised form 11 June 2005; accepted 18 July 2005
Available online 15 September 2005

Abstract

As part of a continuing study pertaining to the use of Fe as a substitute for metals such as Cr and Co in the design and synthesis of metal-complexed azo and formazan dyes, the synthesis of dye ligands containing *ortho*-trifluoroacetamido or mesylamido groups in the diazo components was undertaken. It was anticipated that these groups would mimic the acidity and metallizing properties of an *ortho*-OH group, thus producing new Fe-complexed dyes. The target ligands were synthesized in 4–5 steps and 80–91% yields from commercially available intermediates. ^{1}H NMR was used to confirm the structures of the target dye ligands. The resultant azo and formazan systems readily formed 1:2 Fe-complexes when an *ortho*-$NHSO_2Me$ group was employed, while preparation of Fe-complexes from dye ligands having an *ortho*-$NHCOCF_3$ group proved difficult, with mixtures of unmetallized dye, Fe-complex, and Fe hydroxide obtained despite variations in reaction conditions. Results of DFT calculations suggest that electron density at the N-22 atom was significantly diminished by the electron-withdrawing power of the CF_3 moiety, inhibiting complex formation.

Keywords: Azo and formazan dyes; Iron-complexed dyes; Trifluoroacetamido and mesylamido groups

1. Introduction

The past decade has been marked by a growing interest in the development and use of ecologically friendly dyes. This concept led to the consideration of Fe [1–5] and Al [6–10] salts as metallizing agents and substitutes for metals such as Cr, Co and Ni, with Fe-complexed dyes receiving much of the initial attention.

In previous papers from our laboratories, the synthesis and the technical and mutagenic properties of some Fe-complexed azo and formazan dyes (Figs. 1 and 2) were reported [11–14]. In those reports, it was shown in a number of cases that Fe could be substituted for metals such as Cr and Co without adversely affecting technical and mutagenic properties. While these results suggested that the Fe-complexed analogs were potential replacements for the commercially used Cr and Co prototypes, characterization of the aquatic toxicity of the new dyes was deemed an essential step in their further development. With this point in mind, the *Lemna minor* protocol was used to assess the aquatic toxicity of selected azo and formazan dyes [15]. The results showed that Fe-complexed dyes generally exhibited lower chronic toxicity than the corresponding Cr and Co analogs, before and after ozone treatment. This was consistent with results from experiments showing that the Fe (II) sulfate salt used in dye synthesis had a lower EC_{50} value than its Co and Cr counterparts. It was also apparent that aquatic toxicity correlated with dye–frond affinity before ozone treatment and with pH levels after ozone treatment. In these studies, Cr- and

* Corresponding author. Tel.: +1 919 515 6552; fax: +1 919 515 6532.
E-mail address: harold_freeman@ncsu.edu (H.S. Freeman).

0143-7208/$ - see front matter © 2005 Elsevier Ltd. All rights reserved.
doi:10.1016/j.dyepig.2005.07.009

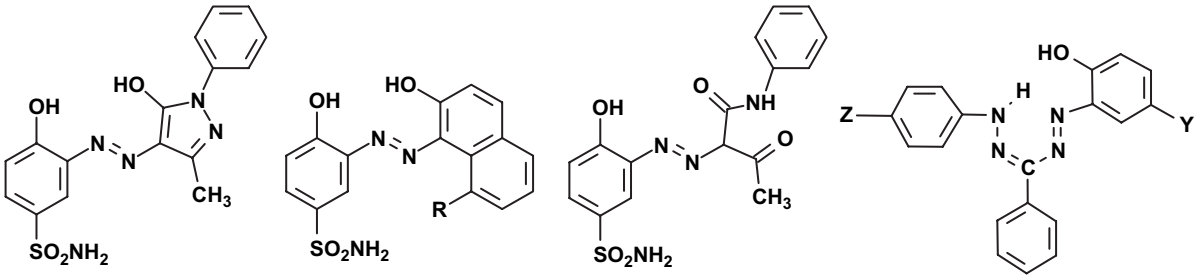

Fig. 1. Structures of some dye ligands used to prepare Fe-complexed dyes [11–14].

Co-complex dyes generally afforded higher levels of dye uptake by fronds (leaves), based on visual inspection, and higher levels of aquatic toxicity than structurally analogous Fe-complexes. The acidity levels in the ozone treated solutions and the rate at which acidity decreased during the test was directly related to increased frond mortality and lower reproduction. While no single structural feature correlated with elevated aquatic toxicity, the azo dyes tended to exhibit higher aquatic toxicity than the formazan dyes.

In more recent studies, the synthesis of monoazo and formazan dyes containing *ortho*-trifluoroacetamido and mesylamido groups in the diazo components was undertaken (cf. **1**–**2**). It was anticipated that these groups would mimic the acidity and metallizing properties of an *ortho*-OH group, thus producing additional families of Fe-complexed dyes.

2. Experimental

2.1. General

The synthesis of dyes was carried out with the use of commercial intermediates from Aldrich Chemical Company (Milwaukee, WI) or Fisher Scientific (Pittsburgh, PA). The progress of reactions was monitored by TLC, using silica gel 60 plates from Aldrich Chemical Company (Milwaukee, WI) and toluene:EtOAc (2:1) or using Alumina B plates from Selecto Scientific (Norcoss, GA) and MeOH.

For molecular modeling studies, structures were generated with the aid of a CAChe graphical editor interface. Formal charges and partial charges were assigned whenever appropriate. A process in the CAChe editor interface called "Beautification" was used to provide a starting structure having standard bond lengths and bond angles, and the correct configuration of each atom in the structure. Lone pairs of electrons and hydrogen atoms were added where appropriate. The equilibrium geometries of dyes **1a**–**b** were located using B88-LYP functional [16, 17] and TZVP basis set [18–20] to conduct DFT (Density Functional Theory) - based calculations implemented in CAChe Worksystem with Degauss 5.0 [21] executed on a 1.7-GHz Pentium 4 computer with 256 MB RAM.

Visible spectra were recorded in EtOH using a Varian Cary 3 UV–visible spectrometer. NMR spectra were recorded using a Bruker AVANCE 500 MHz spectrometer, and FAB mass spectra were recorded using a JEOL HX-110 double focusing mass spectrometer.

2.2. 4-(2′-Aminophenylazo)-1-phenyl-3-methyl-5-pyrazolone (*6a*)

ortho-Nitroaniline (1.38 g, 0.01 mol) was mixed with HCl (2.5 ml, 37%) in a mortar, transferred to a 3-neck round bottom flask, and additional HCl (2 ml, 37%) was added. To the resultant suspension crushed ice (25 g) and $NaNO_2$ (2.5 ml, 4 N) were added. Diazotization was carried out over 0.5 h at 5 °C, and the diazonium salt solution was added dropwise at 5–10 °C to a solution of 1-Phenyl-3-methyl-5-pyrazolone (1.74 g, 0.01 mol) in water (25 ml) containing NaOH (1 ml, 30%) and Na_2CO_3 (1 g). The coupling reaction was stirred overnight, and the pH of the

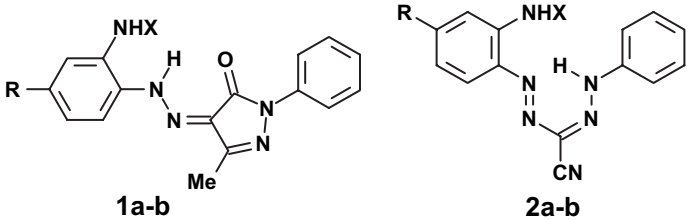

Fig. 2. Structures of dye ligands **1** and **2**, where R = H, Me, CF_3 and X = SO_2Me (a), $COCF_3$ (b).

resultant mixture was adjusted to pH 7 using HCl (6%). The dye was collected, washed with water, and dried. The resultant 4-(2′-Nitrophenylazo)-1-phenyl-3-methyl-5-pyrazolone (**5a**; 3.1 g, 95%) was dissolved in DMF (50 ml) at 55 °C. To this solution, $Na_2S \cdot 9H_2O$ (7.5 g, 0.03 mol) dissolved in H_2O (15 ml) was added and the solution was stirred for 1 h at 60–70 °C. The temperature was reduced to 20 °C, water (200 ml) was added, and sufficient HCl (6%) was added to give pH 5. Dye **6a** was collected by filtration, washed with water, and dried, to give 2.8 g (91%). The coupling and reduction steps were monitored by TLC, using toluene:EtOAc (2:1) as the eluent. R_f (**5a**) = 0.76 and R_f (**6a**) = 0.81.

2.3. 4-(2′-N-methylsulfonylaminophenylazo)-1-phenyl-3-methyl-5-pyrazolone (*1a*)

A solution of 4-(2′-Aminophenylazo)-1-phenyl-3-methyl-5-pyrazolone (2.94 g, 0.01 mol) in pyridine (15 ml) was cooled to 10 °C and stirred as methanesulfonyl chloride (1.2 ml, 0.015 mol) was slowly added. The solution was stirred overnight and poured into an ice/water mixture to precipitate the product. The mixture was stirred for 1 h, filtered, and the product washed with water to give 3.2 g (85%) **1a**. The synthesis was monitored by TLC, using silica gel plates and toluene:EtOAc (2:1). R_f (**1a**) = 0.57.

2.4. 1:2 Fe-complex of dye *1a*

Dye **1a** (3.74 g, 0.01 mol) was dissolved in DMF (20 ml) containing NaOAc (1 g). The mixture was heated to 40 °C and a solution of $FeSO_4 \cdot 7H_2O$ (1.39 g, 0.005 mol) in H_2O (10 ml) was added. The solution was stirred for 1 h and water (100 ml) was added. The mixture was stirred for 3 h, filtered, and the product was washed with water. After drying, 3.75 g (89%) dye was obtained. The synthesis was monitored by TLC using alumina plates and MeOH. R_f (**1a**) = 0.48 and R_f (Fe-complex) = 0.66.

2.5. 4-(2′-N-trifluoroacetamidophenylazo)-1-phenyl-3-methyl-5-pyrazolone (*1b*)

4-(2′-Aminophenylazo)-1-phenyl-3-methyl-5-pyrazolone (2.93 g, 0.01 mol) was dissolved in HOAc (30 ml) at room temperature and trifluoroacetic anhydride (1.4 ml, 0.01 mol) in HOAc (5 ml) was slowly added. The mixture was stirred for 1 h, slowly added to ice/water, and stirred 1 h. The dye was collected, washed with water and dried, to give 3.1 g (91%) product. The synthesis was monitored by TLC using silica gel plates and toluene:EtOAc (2:1). R_f (**1b**) = 0.86.

2.6. 1-(2′-Nitrophenyl)-5-phenyl-3-cyanoformazan (*10a*)

Aniline (0.95 g, 0.01 mol) was dissolved in water (10 ml) containing HCl (3 ml, 30%). Diazotization was effected by the addition of $NaNO_2$ (2.5 ml, 4 N) at 0 °C. The solution was stirred for 15 min and slowly added to a mixture of methyl cyanoacetate (1.1 g, 0.011 mol) in water (10 ml) at room temperature. During this time, the pH of reaction was maintained at 3.6–4.0 by adding saturated NaOAc solution. The mixture was stirred for 1 h, filtered and the product was washed with water. The solid was mixed with water (20 ml) and KOH (3.3 g) dissolved in water (10 ml) was added. The mixture was heated to 80 °C, and kept at this temperature until hydrolysis was complete (monitoring by TLC). The solution of hydrazone **8** was cooled to below 10 °C and acidified (pH 12) using HCl (30%). The diazonium salt of *ortho*-Nitroaniline (1.4 g, 0.01 mol) was prepared as described above for benzenediazonium chloride and then added to the solution of hydrazone, maintaining pH 12 by the addition of NaOH (30%). The reaction was stirred overnight and the product was precipitated by adding HCl (6%) to give pH 7. Dye **10a** was collected, washed with water and dried, to give 17.9 g (91%). The synthesis was monitored by TLC using silica gel plates and toluene:EtOAc (2:1). R_f (**10a**) = 0.86.

The remaining steps reduction, acetylation (mesylation/trifluoroacetylation), and metallization were conducted in the same manner described above for dyes based on 1-Phenyl-3-methyl-5-pyrazolone.

3. Results and discussion

Target azo dye ligands **1** required the synthesis of nitroarylazopyrazolones **5**, reduction of the nitro group of **5**, and subsequent acylation of aminoarylazopyrazolones **6**. Formazan ligands **2** were synthesized in 5 steps. The procedure required coupling compound **8** with diazotized *ortho*-nitroanilines **9**, reduction of intermediates **10**, and acylation of the aminoformazans **11**. The synthetic routes employed to obtain ligands **1** and **2** are shown in Figs. 3 and 4, respectively.

The conversion of dyes **1** and **2** to their 1:2 Fe-complexes was conducted in DMF/H_2O, using Fe (II) sulfate in the presence of NaOAc, and the products were isolated by triturating with H_2O. The yields and key physical properties of ligands **1** and **2**, and their 1:2 metal complex are summarized in Tables 1 and 2. These results indicate that azo and formazan dyes **1a** and **2a** readily formed 1:2 Fe-complexes. However, the preparation of Fe-complexes of **1b** and **2b** proved difficult, with mixtures of unmetallized dye, Fe-complex, and Fe hydroxide obtained regardless of the reaction times or temperatures employed. Results from molecular

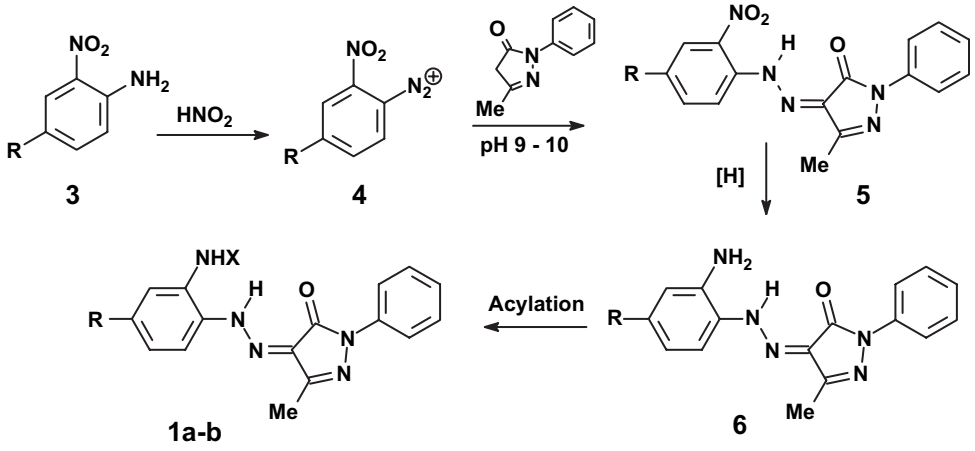

Fig. 3. Four-step synthesis of dyes **1a–b** (X = SO_2Me, $COCF_3$ and R = H, Me, CF_3).

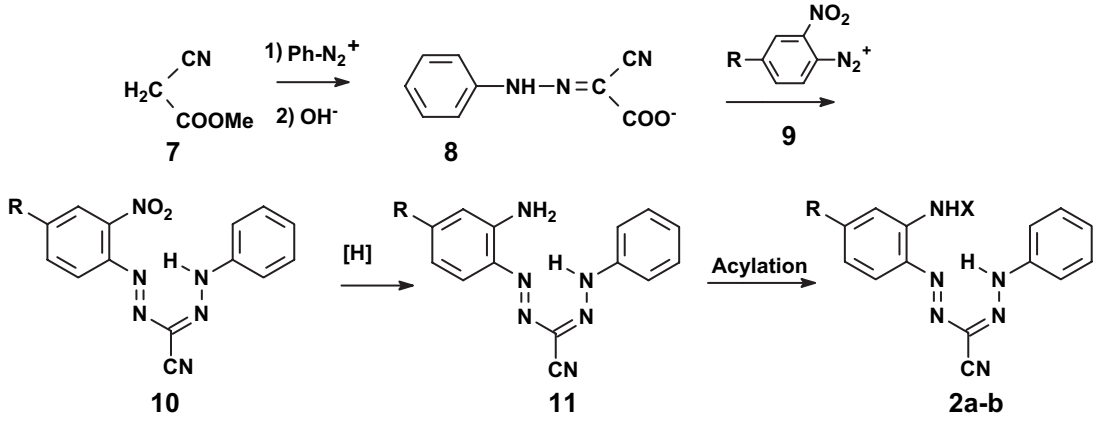

Fig. 4. Five-step synthesis of dyes **2a–b** (X = SO_2Me, $COCF_3$ and R = H, Me).

Table 1
Yields, mp and absorption data for azo dyes **1a** (X = SO_2Me) and **1b** (X = $COCF_3$)

Dye	R	*N*-mesyl (trifluoroacetyl) ligand				1:2 Fe-complex		
		Yield (%)	Mp (°C)	λ_{max}[a]	$\varepsilon \times 10^{-4}$	Yield (%)	λ_{max}[a]	$\varepsilon \times 10^{-4}$
1a (**1b**)	H	85 (84)	228–230 (241–242)	392 (394)	2.33 (2.51)	89 (–)	422 (–)	2.69 (–)
	Me	87 (84)	234–236 (251–252)	400 (402)	1.96 (2.44)	84 (–)	424 (–)	3.08 (–)
	CF_3	91 (87)	236–238 (254–256)	409 (390)	2.05 (2.54)	86 (–)	429 (–)	3.36 (–)

[a] Recorded in EtOH.

Table 2
Yields, mp and absorption data for formazan dyes **2a** (X = SO_2Me) and **2b** (X = $COCF_3$)

Dye	R	*N*-mesyl (trifluoroacetyl) ligand				1:2 Fe-complex		
		Yield (%)	Mp (°C)	λ_{max}[a]	$\varepsilon \times 10^{-4}$	Yield (%)	λ_{max}[a]	$\varepsilon \times 10^{-4}$
2a (**2b**)	H	89 (83)	198–203 (208–212)	452 (440)	1.95 (2.01)	85 (–)	481 (–)	2.13 (–)
	Me	80 (83)	219–222 (221–225)	448 (437)	2.04 (2.13)	97 (–)	479 (–)	2.31 (–)

[a] Recorded in EtOH.

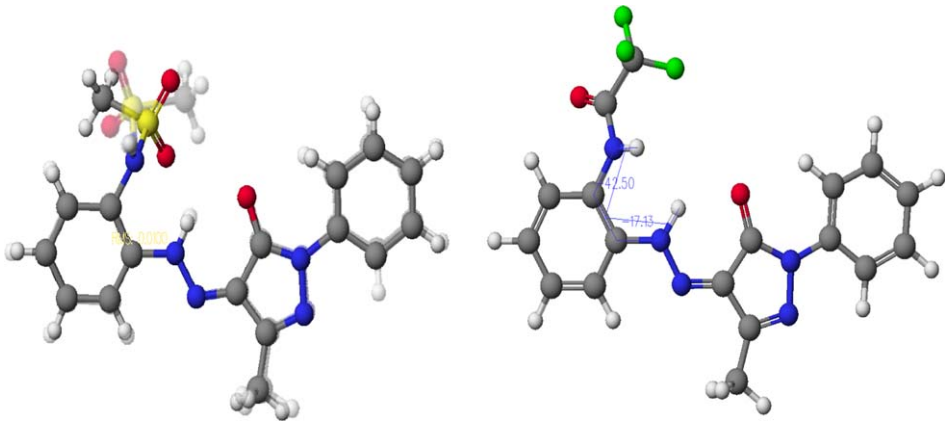

Fig. 5. Structures for **1a–b** (R = H), where X = SO_2Me (left) and $COCF_3$ (right). For X = SO_2Me the X-ray structure is in the front and the calculated structure in the background.

modeling studies using semi-empirical methods [16] to study dye **1b** suggested that the optimized structure has the N–H moiety twisted out of position for metal complex formation. Subsequently, we found that DFT-based calculations gave improved results. In this regard, it can also be seen from Fig. 5 and Table 3 that the DFT-calculated structure for **1a** was validated by X-ray crystallography. It is also evident from the results in Table 3 that the 5 key torsion angles in **1a** and **1b** are not significantly different. Hence, it is very likely that factors other than geometry influenced Fe-complex formation. With this point in mind, we examined the electronic properties of the N-22 atom. Results of DFT calculations showed that the partial charge on the N-22 was −0.716 for ligand **1a** versus −0.388 for ligand **1b**. This significant difference in partial charges suggests that electron density at N-22 was significantly diminished by the electron-withdrawing power of the CF_3 moiety, inhibiting complex formation.

Table 3
Comparison of experimental (X-ray) and calculated (DFT) torsion angles for dye **1**

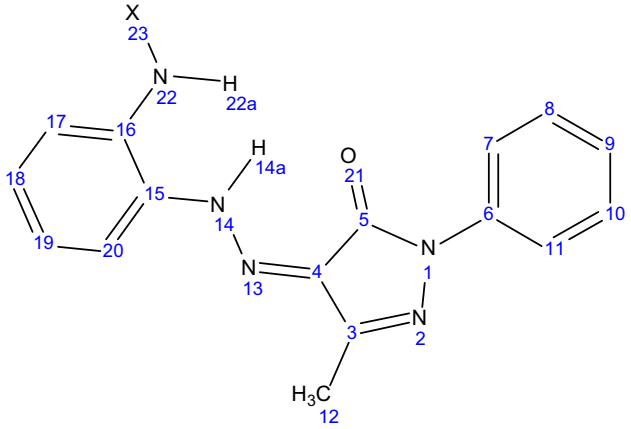

Torsion angle (°)	**1a** (X = SO_2Me)		**1b** (X = $COCF_3$)
	X-ray	DFT	DFT
15-16-22-22a	−123.74	−117.3	42.5
20-15-14-13	−13.25	−14.94	4.15
14a-14-13-4	−2.83	−4.29	1.57
21-5-4-13	0.40	1.57	4.66
14a-14-15-16	−7.77	−12.005	−17.13

^{1}H NMR data used to confirm the structures of the target dye ligands are shown in Table 4. Compounds **1a–b** were characterized by the expected hydrazone forms, as judged by the broad peak at δ13.3 ppm. In each case the NH protons for the $MeSO_2NH-$ moiety gave a broad peak near δ9.50 ppm. For the sake of brevity, entries for the ring protons are designated as multiplets (m), while in actuality the expected combinations of singlets, doublets and triplets were observed for the aromatic systems. For instance, the spectrum for dye **1a** (R = H, X = SO_2Me) had doublets at 7.9, 7.85, 7.4, and 7.25 ppm, with overlapping triplets at 7.45 and 7.25 ppm as shown in Fig. 6.

Negative ion FAB mass spectrometry was employed to support the chemical structures of Fe-complexed dyes. In each case a weak molecular ion $[M]^{\bullet}$ peak and a strong pseudo molecular ion $[M - Na]^-$ peak were detected. The relative abundances are summarized in Table 5 and a representative spectrum is shown in Fig. 7.

Incorporating an Fe-atom into dyes caused a 20-nm bathochromic shift in λ_{max}, along with broadening of the absorption band and an increase in ε_{max}. See for instance, the Fe-complex and unmetallized form of **1a** in Fig. 8.

Table 6 shows typical lightfastness data obtained after 2% solutions of these solvent dyes were applied to paper and given a 170-kJ exposure to xenon arc light in

Table 4
^{1}H NMR (300 MHz) data for dyes **1a–b** and **2a** in DMSO

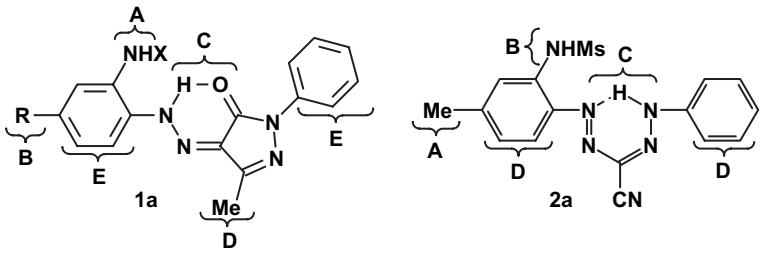

Dye	R	^{1}H NMR – δ (ppm)				
		A	B	C	D	E
1a	H	3H, s, δ3.1; 1H, s, δ9.6	With E	1H, bs, δ13.8	3H, s, δ2.3	9H, m, δ7.2–7.9
1a	Me	3H, s, δ3.1; 1H, s, δ9.4	3H, s, δ2.2	1H, bs, δ13.6	3H, s, δ2.3	8H, m, δ7.1–7.9
1b	H	–	With E	1H, bs, δ13.2	3H, s, δ2.3	9H, m, δ7.3–7.9
1b	Me	–	3H, s, δ2.2	1H, bs, δ13.3	3H, s, δ2.2	8H, m, δ7.0–7.9
2a	H	3H, s, δ2.4	3H, s, δ3.6; 1H, s, δ9.5	1H, s, δ12.8	8H, m, δ7.3–7.8	–

a standard weatherometer. For both dye types, the best results were obtained when R = H.

4. Conclusions

We found that Fe-complexed *N*-mesylarylazo-1-phenyl-3-methyl-5-pyrazolone-based azo dyes exhibited good color strengths and light fastness, but the colors obtained were limited to yellow-brown shades (λ_{max} = 390–402 nm). On the other hand, the application properties for the corresponding formazan dyes were much less than ideal, as color strength and light fastness were reduced by substituting an *ortho*-$NHSO_2Me$ group for an –OH group. It is also clear that the present azo and formazan dye ligands are not

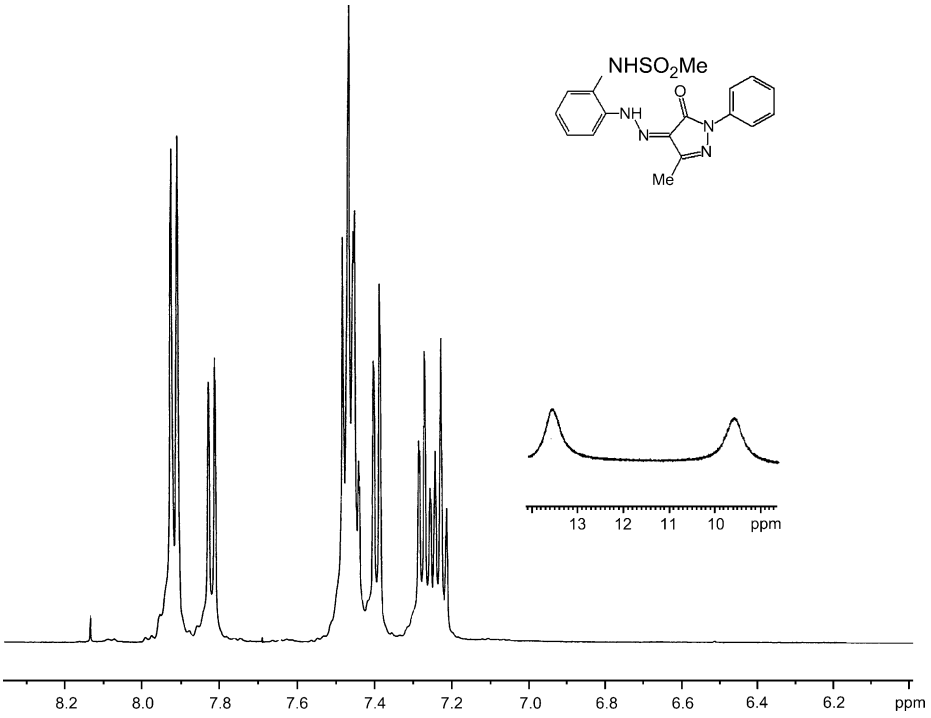

Fig. 6. ^{1}H NMR spectrum for dye **1a** (R = H, X = SO_2Me).

Table 5
Relative abundances of molecular ion species in FAB mass spectra of 1:2 Fe-complexed dyes

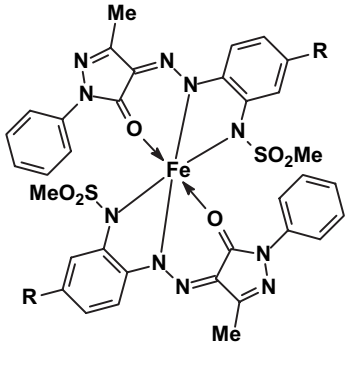

1:2 Fe complex of 1a

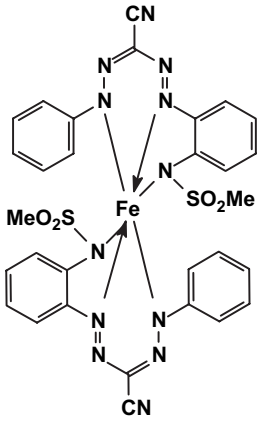

1:2 Fe complex of 2a

1:2 Fe-Complex of	R	FAB		
		Assignment	*m/z*	Rel. Int.
1a[a]	H	$[M]^{\cdot}$	817	10
		$[M - Na]^{-}$	794	100
1a[b]	Me	$[M]^{\cdot}$	845	5
		$[M - Na]^{-}$	822	48
1a[b]	CF_3	$[M]^{\cdot}$	899	7
		$[M - Na]^{-}$	876	43
2a[b]	H	$[M]^{\cdot}$	759	12
		$[M - Na]^{-}$	736	61

[a] Relative ion abundances are based on the matrix peak at $m/z = 305.2$ (3-nitrobenzyl alcohol, 100%).
[b] Relative ion abundances are based on the matrix peak at $m/z = 459.2$ (3-nitrobenzyl alcohol, 75%).

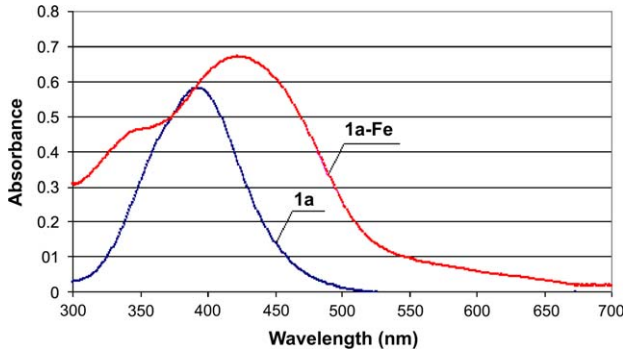

Fig. 8. Absorption spectra for dye **1a** (R = H, X = SO_2Me) and its 1:2 Fe-complex.

amenable to Fe-complex formation when an *ortho*-$NHCOCF_3$ group replaces an *ortho*-OH group.

Acknowledgement

This work was supported through a grant from Clariant Corporation, Huningue Cedex, France, and the collaboration of Drs. Bansi Kaul, Hans Joachim Metz, and Dominique Pflieger is gratefully acknowledged.

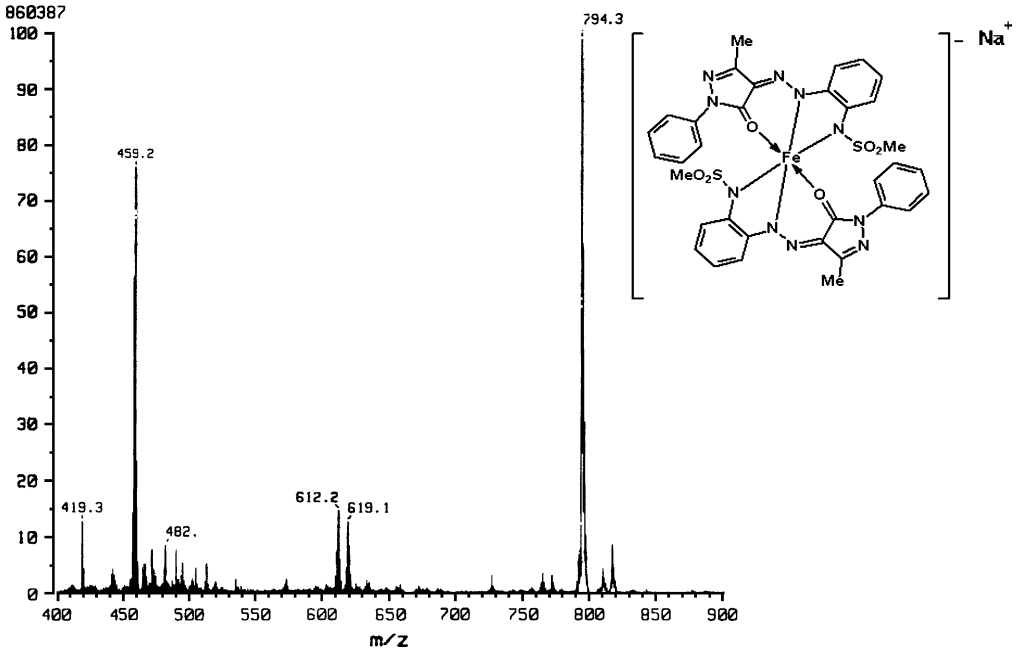

Fig. 7. FAB mass spectrum of Fe-complex of **1a** (R = H, X = SO_2Me).

Table 6
Lightfastness data for metal complex of dyes **1a** and **2a**

Dye	Metal	Class	Color	ΔE	GS value	GS rating[a]
1a (R = H)	Fe	Azo	Brown	1.58	4.32	4–5
1a (R = Me)	Fe	Azo	Brown	2.16	3.97	4
1a (R = CF_3)	Fe	Azo	Brown	3.76	3.02	3
2a (R = H)	Fe	Formazan	Brown	0.02	4.99	5

[a] Follows a 170-kJ xenon arc exposure. Gray scale (GS) rating − 5 (highest) − 1 (lowest).

References

[1] Bardole HA, Freeman HS, Reife A. Text Res J 1998;68(2):141.
[2] Freeman HS, Sokolowska-Gajda J, Reife A, Claxton LD, Houk VS. Text Chem Color 1995;27(2):13.
[3] Czajkowski W, Szymczyk M. Dyes Pigments 1998;37(3):197.
[4] Julia MR, Munoz I, Erra P. Melliand TextBer 1993;74(11):1161.
[5] El-Shishtawy RM, Kamel MM. Chem Eng Technol 2002;25(8):849.
[6] Kaul BL, Pflieger D. Clariant Finance (BVI) Ltd., USP 5698683; 1997.
[7] Rao TVRK, Kumud SNP. J Inst Chem 2001;73(4):143.
[8] Lycka A, Lustinec D, Holecek J, Nadvornik M, Holcapek M. Dyes Pigments 2001;50(3):203.
[9] Yang L, Zhang L, Lu Y. Chinese P 1125743; 1996.
[10] Lycka A, Rys P, Skrabal P. Magn Reson Chem 1998;36(4):279.
[11] Sokolowska-Gajda J, Freeman HS, Reife A. Text Res J 1994;64(7):388.
[12] Freeman HS, Sokolowska-Gajda J, Reife A. Text Chem Color 1995;27(2):13.
[13] Sokolowska-Gajda J, Freeman HS, Reife A. Dyes Pigments 1996;30(1):1.
[14] Edwards LC, Freeman HS, Claxton LD. Mutat Res 2004;546(1–2):17.
[15] Edwards LC. The aquatic toxicity and mutagenicity of azo and formazan dyes, PhD dissertation, North Carolina State University, Fiber and Polymer Science Program; 1996.
[16] Becke D. J Chem Phys 1988;88:1053.
[17] Lee C, Yang W, Parr RG. Phys Rev B 1988;37:785.
[18] Dunning Jr TH. J Chem Phys 1971;55:716.
[19] McLean AD, Chandler GS. J Chem Phys 1980;72:5639.
[20] Ahlrichs R, Taylor PR. J Chem Phys 1981;78:315.
[21] CAChe Worksystem 3.6, Oxford Molecular Group, Box 4003, Beaverton, OR 97076; 1993.